Excess-noise-enhanced parametric down conversion

Claus Lamprecht,[1,2] Murray K. Olsen,[2] Matthew Collett,[2] and Helmut Ritsch[1]
[1]*Institut für Theoretische Physik, Universität Innsbruck, Technikerstr. 25, A-6020 Innsbruck, Austria*
[2]*Department of Physics, University of Auckland, Private Bag 92019, Auckland, New Zealand*
(Received 8 February 2001; published 14 August 2001)

We calculate the influence of excess noise on parametric down conversion in an unstable optical parametric oscillator (OPO), using a quantum quasimode description. We find a strongly enhanced pair photon generation rate below threshold as compared to a conventional stable cavity setup of comparable gain and loss. In addition, the oscillation threshold is lowered due to the influence of the excess noise and the squeezing properties of the emitted light are significantly changed. In general, the maximal quantum-noise suppression in one quadrature component is reduced, which poses strong limitations for the practical usefulness of a geometrically unstable OPO source. The analytical results from our quasimode description are in good agreement with numerical simulations using a positive-*P* representation of the field in mode space and in position space.

DOI: 10.1103/PhysRevA.64.033811 PACS number(s): 42.65.Yj, 42.50.Lc

I. INTRODUCTION

The optical parametric oscillator is one of the most thoroughly theoretically investigated and successfully experimentally used tools in modern quantum optics. Applications range from the generation of squeezed light and quantum-correlated twin beams to multiphoton entangled states. The generated light fields can be used for purposes such as high-resolution spectroscopy, tests for violation of Bell's inequalities, and demonstration of quantum teleportation [1]. The process of optical parametric down conversion is in general well understood theoretically [2–5]. Some well-proven model Hamiltonians describing the essentials of the system dynamics have been found and yield very good agreement between prediction and experimental verification. The fundamental process in these models is the generation of quantum entangled pairs of a signal and an idler photon from a single-pump photon through the nonlinear medium. Below oscillation, threshold down conversion has been found to be a genuine quantum noise-driven process with no classical counterpart, similar to spontaneous emission or nuclear decay.

In contrast to this success for stable cavity geometries, the situation in quantum optics systems based on an unstable geometry, e.g., an unstable cavity laser, is completely different. Although the basic concepts of the phenomenon of excess noise were laid down by Petermann more than 20 years ago [6] and have been tested for decades, there are still some mysteries and a fundamental quantum-mechanical description has been difficult. One fact is that the linewidth of an unstable cavity laser is considerably larger than the linewidth of a stable cavity laser with equal gain and loss properties, in contradiction to the Schawlow-Townes rule. This effect was attributed to the nonorthogonality of the cavity modes [7] and amplified spontaneous emission. Some decisive tests of this property were carried out 20 years ago [8].

Recently, more refined experiments have clearly demonstrated a geometry-dependent laser linewidth, which could be well accounted for by the so-called Petermann excess-noise-factor K [9–11]. As a consistent quantum description of this phenomenon starting from first principles was missing, renewed theoretical interest in the origin and interpretation of this rather counterintuitive phenomenon [12–14] has arisen.

In our theoretical description of the microscopic origin of excess noise [15,16], we looked at a simple genuine quantum system, namely, a single excited two-level atom, and investigated the influence of excess noise on spontaneous emission. To this end, we developed an approximate quantum description, where the field operators were expanded in either the cavity matched or the adjoint quasimodes. With this approach, we were able to discuss the origins and limitations of the K-factor approach. In the special case of an active system, we recovered the K-fold-enhanced laser linewidth, whereas for a single atom inside an empty unstable cavity, a more thorough approach must be taken. In parallel, various alternative quantum descriptions of excess noise in lasers (active systems) [12,13] were developed, which more or less confirmed the previously obtained results. These treatments are based on descriptions using a finite set of normalizable orthogonal ''modes of the universe.'' Here, the spatially dependent gain and loss implies a coupling to the empty cavity modes, which can then be identified as the origin of the excess noise. It is, however, not obvious how to apply these models to geometrically unstable situations, where no closed optical path exists for the lasing mode. An alternative proposal was to dynamically include the mirrors in the model as a set of damped dipoles and explicitly solve the resulting coupled set of equations [17]. Although this approach needs only few limiting assumptions, the procedure gets rather complicated in practice.

It is now quite natural to develop the picture of excess noise further and investigate other genuine quantum noise-driven processes. In this article, we apply our quasimode strategy to spontaneous twin-photon generation as a paradigm of a *nonlinear* quantum noise-driven process. In the limiting case of operation well below threshold, adiabatic elimination of the pump mode enabled us to derive analytical solutions for the dynamics of an unstable cavity optic parametric oscillator (OPO) using a nonorthogonal quasimode basis set [18]. We found features that were strongly dependent on the excess noise, such as an enhanced intensity and

modified photon correlations. Furthermore, it turned out that excess noise destroyed the squeezing of the subharmonic beam. An enhanced twin-photon generation rate in a stable resonator was recently also experimentally demonstrated [19] at the expense of a prolonged photon coincidence interval (narrower band width of the emitted photons).

In this paper we will also explore the behavior above threshold. For this we must resort to numerical simulations. Since our expansion in matched and adjoint mode pairs gives rise to different left- and right-field eigenstates, the phase-space method we use has to include nondiagonal coherent state projection operators. As a possible candidate, we have chosen the positive-P representation [20,21] to perform the simulations. Below threshold we can compare our results with previous analytical predictions [18], finding excellent agreement. In a further step to consolidate these results we also compare them to quantum simulations in real space [5], which do not rely on any choice of mode expansion, and hence, give an independent test.

Extending the simulations to stronger pump amplitudes, we find an enhancement of the average intensity as well as a lowering of the threshold of oscillation. Calculating the spatial field distribution, we find destructive interference with the higher-order mode contributions that gives rise to a reduced beam width. Interestingly, we find a surprising plateau in the two-photon coincidence count rate for rather short times.

II. QUANTUM QUASIMODE ANALYSIS

For the purposes of making this paper self-contained, let us first recall some key aspects of the quasimode expansion for an unstable cavity as developed in Ref. [16]. Within the paraxial approximation, the quasimodes $u_n(\mathbf{x},0)$ fulfill a self-reproducing condition after one round trip, i.e., the so-called *matched modes* $u_n(\mathbf{x},0)$ are eigenfunctions of the underlying Huygens' integral kernel $K(\mathbf{x},\mathbf{x}')$ [22]

$$\int d\mathbf{x}' K(\mathbf{x},\mathbf{x}') u_n(\mathbf{x}',0) = \gamma_n u_n(\mathbf{x},0). \tag{2.1}$$

For geometrically unstable systems this operator is not Hermitian and the quasimodes are no longer orthogonal. Nevertheless, there exists a biorthogonal set of adjoint modes $v_n^*(\mathbf{x},z)$ (eigenfunctions of K^T), i.e., $(u_n,v_m)=\delta_{nm}$, where $(.,.)$ denotes the transverse integral. For any transversely finite system, the matched modes can be normalized to unity, i.e., $(u_n,u_m)=A_{nm}$ with $A_{nn}=1$. In contrast to this, the norm of the adjoint modes contains the Petermann excess noise factor K_n, i.e., $(v_n,v_m)=B_{nm}$ with $B_{nn}=K_n$. In this case these modes are complete and fulfill $\Sigma_n v_n^*(\mathbf{x})u_n(\mathbf{x}')=\delta(\mathbf{x}-\mathbf{x}')$. For any symmetric mirror setup ($K^T=K$) the adjoint modes are proportional to the matched modes $v_n^*(\mathbf{x})=\sqrt{K_n}u_n(\mathbf{x})$ at the symmetry plane.

Unfortunately, in general, the quasimodes cannot be explicitly calculated analytically. There do exist, however, some exceptions for which they can be found. An important example of an analytically soluble model is a resonator of length L consisting of two symmetric spherical mirrors of focal length f and Gaussian reflectivity profile with width L_G. Restricting ourselves to the paraxial approximation and one transverse spatial dimension, we find complex Hermite-Gaussian mode functions for the transverse field modes at the symmetry plane $z=0$: (cf. [23])

$$u_n(x) = c_n H_n(p_0 x) e^{[-i(k_n)/(2R0)]x^2} e^{-(x^2/w0^2)}, \tag{2.2}$$

$$v_n(x) = \tilde{c}_n H_n(p_0^* x) e^{[i(k_n)/(2R0)]x^2} e^{-(x^2/w0^2)}. \tag{2.3}$$

Here, $w_0=(2z_0/k_n)(1+r_0^2/z_0^2)$ is the beam width, $R_0=r_0[1+(z_0^2/r_0^2)]$ is the radius of curvature with transverse scaling $p=\sqrt{ik_n/q_0}$ and H_n denotes the nth Hermite polynomial. The coefficients $c_n,\tilde{c}_n$ are fixed by the normalization constraints discussed above. Further, one finds for the quasimode eigenvalues $\gamma_n=[(q_0-L/2)/(q_0+L/2)]^{(2n+1)} \equiv e^{-(\kappa_n+i\omega_n)(2L/c)}$ giving explicit expressions for the frequencies and loss rates. The only remaining free parameter is the complex source point $q_0=L/2\sqrt{1-4/l}\equiv r_0+iz_0$, which is directly linked to the cavity parameters; $l=L/f+i/N$ and $N=\pi L_G^2/\lambda L$ would be the Fresnel number of a corresponding hard-edged spherical mirror. For $0<L/f<4$, the resonator is stable and $u_n(x)$ are simply the well-known Hermite-Gaussian modes.

Outside this interval for f, the resonator is geometrically unstable and these quasimodes correspond to eigenfunctions of the inverted harmonic-oscillator potential [24]. Although this type of resonator setup might not be very typical, it has the twin advantages of explicit analytical solubility and a continuous transition from the stable to the unstable case connecting it to well-known and proved results.

Let us now turn to field quantization. Since these mode pairs fulfill a completeness relation, every field distribution can be expanded uniquely either in the matched modes or in the adjoint modes. For our purpose it proves advantageous to expand the field operators (positive and negative frequency part of the vector potential) in the following way:

$$A(\mathbf{x},t) = \sum_n a_n(t) u_n(\mathbf{x}), \tag{2.4}$$

$$A^\dagger(\mathbf{x},t) = \sum_n b_n^\dagger(t) v_n^*(\mathbf{x}), \tag{2.5}$$

where $a_n(t), b_n^\dagger(t)$ are generalized creation or annihilation operators for the corresponding matched and adjoint mode pairs. This becomes obvious if we rewrite the canonical equal-time commutation relations [25] in terms of these operators:

$$[a_n, b_m^\dagger] = \delta_{nm}, \tag{2.6}$$

$$[a_n, a_m^\dagger] = B_{nm}, \tag{2.7}$$

$$[b_n, b_m^\dagger] = A_{nm}. \tag{2.8}$$

Obviously the sets of operators (a_n,b_n) are not independent and we find

$$b_n = \sum_m A_{nm} a_m , \tag{2.9}$$

$$a_n^\dagger = \sum_m B_{mn} b_m^\dagger . \tag{2.10}$$

Using this field expansion the free-field Hamiltonian can be written in the form

$$H_F = \sum_{nm} \hbar \frac{\omega_n + \omega_m}{2} A_{mn} a_m^\dagger a_n , \tag{2.11}$$

where the frequencies ω_n are determined from the mode eigenvalues γ_n. As we are dealing with an open system (Gaussian aperture) the mode amplitudes decay exponentially with a mean rate κ_n. Physically, a fraction of the energy is scattered into the continuum modes outside the cavity. In a proper quantum treatment, loss can be modeled by input-output couplings [26] to external reservoirs (heat baths). Alternatively, we could include the field outside the resonator into the Hamiltonian [17]. The second explicit procedure is rather involved for our case, since the scattering losses transverse to the cavity axis are not negligible. As far as the mean mode dynamics is concerned, they are indistinguishable from the losses due to mirror transmission [even for perfect mirrors ($L_g \to \infty$) the loss rate γ_n stays finite in the unstable case]. Tracing over the reservoirs and using a Markov approximation in the first approach will give a master equation for the mode dynamics. However, a satisfactory derivation of this master equation is, to our knowledge, not known for unstable resonators or might even be impossible [14].

Nevertheless, consistency of the effective time evolution for the field density operator is guaranteed if one uses the following ansatz for the master equation:

$$\dot{\rho}_F = -\frac{i}{\hbar}[H_F, \rho_F] + \sum_{nm} A_{nm} \{ (\kappa_n + \kappa_m) a_n \rho_F a_m^\dagger - \kappa_n a_m^\dagger a_n \rho_F - \kappa_m \rho_F a_m^\dagger a_n \} . \tag{2.12}$$

Note that this master equation is of the Lindblad form and represents the only consistent way, within the Markov approximation, to yield the exponential damping of the field modes, i.e., $\dot{a}_n \sim -\kappa_n a_n$. In practice, we will make use of stochastic differential equations for the field operators themselves rather than solving this master equation. That means that for the positive P representation just the exponential mode damping turns out to be important. Let us, however, mention at this point that although looking rather intuitive here, the validity of a master equation treatment can be doubtful if the system is too strongly coupled to the reservoir. As has been suggested recently, this can be the case for significantly unstable resonators [14] or for very small apertures.

III. UNSTABLE CAVITY OPO

To concentrate on the main physical aspects, we restrict ourselves to an analytically soluble case and consider degenerate parametric down conversion with a thin crystal (thin crystal assumption [27]) in a symmetric unstable resonator. In principle, this can be generalized to longer crystals but as long as no transverse changes are introduced, we do not expect significant qualitative changes. We further assume a uniform plane-wave pump field A_P of frequency ω_P interacting with the intracavity field (subharmonic modes) via a $\chi^{(2)}$ medium. Generalizing previous quantum treatments of the transverse dynamics in an OPO [2,3,5] we will concentrate here on the effects of excess noise. The basic Hamiltonian can be separated into four parts:

$$H = H_F + H_P + H_{ext} + H_{int} , \tag{3.1}$$

with

$$H_P = \hbar \omega_P A_P^\dagger A_P , \tag{3.2}$$

$$H_{ext} = i(A_P \varepsilon_{in}^* - A_P^\dagger \varepsilon_{in}), \tag{3.3}$$

$$H_{int} = \frac{i\hbar g}{2} \int d\mathbf{x} [A_P A(\mathbf{x},t)^{\dagger 2} - A_P^\dagger A(\mathbf{x},t)^2], \tag{3.4}$$

where ε_{in} is the pump strength, g is the coupling constant and the integral extends over the volume of the nonlinear medium, which is assumed to be transversally very large compared with the mode width w_0. In terms of the quasimodes, as described in the previous section, we find that the relative coupling strengths are given by the integrals $\int d\mathbf{x} u_n(\mathbf{x}) u_m(\mathbf{x})$ and $\int d\mathbf{x} v_n^*(\mathbf{x}) v_m^*(\mathbf{x})$, respectively. The symmetry of the resonator implies $v_n^*(\mathbf{x}) = \sqrt{K_n} u_n(\mathbf{x})$, and hence, the interaction becomes diagonal due to the biorthogonality of the quasimodes. After some algebra, we find

$$H_{int} = \frac{i\hbar g}{2} \sum_n \left(A_P \sqrt{K_n} b_n^{\dagger 2} - \frac{A_P^\dagger}{\sqrt{K_n}} a_n^2 \right). \tag{3.5}$$

Note that although each of the individual terms of this sum is not explicitly Hermitian and shows formal asymmetry between photon production and annihilation, the total Hamiltonian is Hermitian. Nevertheless, from this way of writing the Hamiltonian we may already expect enhancement of the two-photon generation rate via the excess noise. In principle, the choice to expand the fields in this way is arbitrary, but will prove to be very useful for the subsequent calculations. Finally, the pump-field losses κ_P are treated by the standard reservoir coupling to give

$$\dot{\rho}_P = -\frac{i}{\hbar}[H_P, \rho_p] + \kappa_P (2 A_P \rho_P A_p^\dagger - A_p^\dagger A_P \rho_P - \rho_P A_P^\dagger A_P). \tag{3.6}$$

IV. POSITIVE-*P* SIMULATION OF THE INTRACAVITY FIELD DYNAMICS

In general, the solution for the quantum dynamics induced by the above Hamiltonian cannot be found analytically. Hence, we have to resort to numerical techniques. For this we will employ the well-established method of representing the field by a positive-*P* function [20] and solving the corresponding stochastic differential equations equivalent to the Fokker-Planck equation. The Glauber *P* representation is not useful for simulation of this system since the resulting Fokker-Planck equation has a nonpositive diffusion matrix. Similarly, due to the large number of modes involved, a Wigner function approach would converge only slowly. Let us emphasize here that by choosing the positive-*P* representation, only normally ordered field-expectation values enter into the noise correlations. Hence, the vacuum noise in the reservoir does not explicitly enter into the simulation dynamics and we only get field-dependent noise sources stemming from the nonlinearity of the Hamiltonian. This also strongly simplifies the treatment of a spatially varying damping.

Similar to the orthogonal mode case, a generalized positive-*P* representation may be introduced as the expansion of a given density operator in nondiagonal coherent state projection operators [20,28]. The main difference is that the operators $b_n^\dagger$ here play the role of the usual creation operators $a_n^\dagger$ in an orthogonal basis. After some algebra we find the following stochastic differential equations for the independent variables $\alpha_n, \alpha_n^+, a_P, a_P^+$ corresponding to the quasimode operators $a_n, a_n^\dagger, A_P, A_P^\dagger$, i.e.,

$$\dot{\alpha}_n = -(\kappa_n - i\Delta_n)\alpha_n + g a_P \sqrt{K_n} \sum_m A_{mn}\alpha_m^+ + \sqrt{g a_P \sqrt{K_n}}\, dV_n,$$

$$\dot{\alpha}_n^+ = -(\kappa_n + i\Delta_n)\alpha_n^+ + g a_P^+ \sqrt{K_n} \sum_m A_{nm}\alpha_m + \sqrt{g a_P^+ \sqrt{K_n}}\, dW_n,$$

$$\dot{a}_P = -\kappa_P a_P - g/2 \sum_n \alpha_n^2/\sqrt{K_n} + \varepsilon_{in},$$

$$\dot{a}_P^+ = -\kappa_P A_P^+ - g/2 \sum_n \alpha_n^{+2}/\sqrt{K_n} + \varepsilon_{in}^*, \qquad (4.1)$$

where $\Delta_n = \omega_n - \omega_P/2$ denotes the detuning and dV_n, dW_n are independent Wiener noise increments [26] satisfying $\langle dV_n dV_m\rangle = \langle dW_n dW_m\rangle = \delta_{nm}, \langle dV_n dW_m\rangle = 0$. The first obvious but not unexpected difference from the conventional stable cavity equations [2,3,5] is that the individual mode equations are no longer independent for nonorthogonal modes. The second very interesting difference is the increased noise strength amplified by a factor of $\sqrt{K_n}$ (cf. [17,29]). Similar to the fact that spontaneous emission into the lasing mode of, for example, unstable gain-guided lasers is directly enhanced by the excess-noise factor [6,7,15], we find an increased noise intensity in our system. This lends support to the interpretation of excess noise as a local enhancement of the vacuum quantum fluctuations.

V. SINGLE-MODE APPROXIMATION

Starting from these equations, let us first restrict ourselves to the simplest possible case and consider only a single-mode index *n*. Below threshold, there is actually no good justification for such a truncation, but in the oscillation regime above threshold, one can expect only the lowest loss mode to be significantly excited, as it is true for the stable case. If we neglect all other amplitudes and restrict ourselves to the weak-coupling regime, where the expectation values can be factorized, we find the following analytical expressions for the steady-state intensity (intracavity photon number) [33]:

$$I_P = \langle A_P^\dagger A_P\rangle_{ss} = \frac{\kappa^2 + \Delta^2}{K g^2},$$

$$I_S = \langle a^\dagger a\rangle_{ss} = \frac{2\kappa_P\sqrt{\kappa^2+\Delta^2}}{g^2}\left(\frac{|\varepsilon_{in}|}{\varepsilon_{th}} - 1\right), \qquad (5.1)$$

with

$$\varepsilon_{th} = \frac{\kappa_P\sqrt{\kappa^2+\Delta^2}}{\sqrt{K} g}. \qquad (5.2)$$

Obviously, this gives a significantly lower oscillation threshold for the OPO and an increase in the probability of down conversion by the excess-noise-factor *K*. Of course, in practice one needs a much stronger pump in unstable cavity geometries to achieve a comparable intracavity intensity due to the usually larger losses κ, κ_p. Nevertheless, it may be possible to find a system with large excess noise and relatively low loss rates using hard apertures or small holes in the mirrors, where diffraction plays an important role [18].

VI. TWO-PHOTON GENERATION BELOW THRESHOLD

Let us now return to the full coupled multimode equations. For sufficiently weak pumping (well below threshold) we can linearize our equations, neglect pump depletion, and adiabatically eliminate the pump dynamics from the system. As in the stable cavity case [5], the resulting field amplitudes and intensities in this limit can be calculated analytically [18], with the pump field fixed to its steady-state value $A_{ss} = \varepsilon_{in}/\kappa_p$. After some calculations, we find the following formula for the intracavity field intensity (photon number):

$$I_{ss}(x) = \sum_{nm} \langle a_n^\dagger a_m\rangle u_n^* u_m = \sum_{nm} f_{nm} B_{mn} u_n^* u_m, \qquad (6.1)$$

with

$$f_{nm} = \int \frac{d\omega}{2\pi} \frac{\epsilon_0^2(\kappa_n + \kappa_m)}{[\epsilon_0^2 - \Delta_n^2 - (\kappa_n + i\omega)^2][\epsilon_0^2 - \Delta_m^2 - (\kappa_m - i\omega)^2]} \qquad (6.2)$$

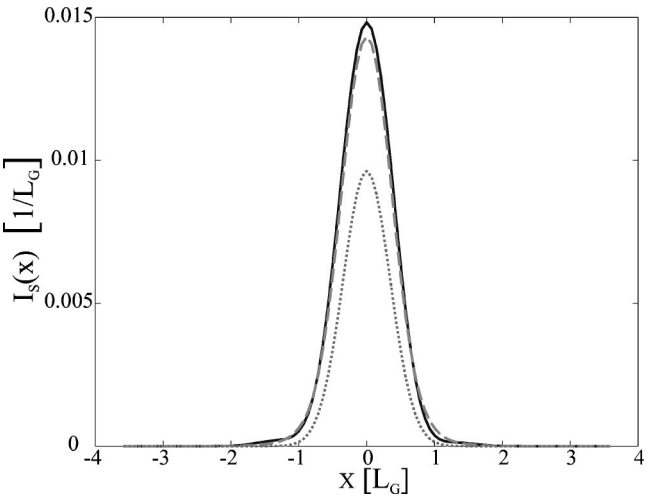

FIG. 1. This picture compares the spatial signal intensity $I(x)$ calculated using the positive-P representation (solid line) with the analytical solution Eq. (6.1) (dashed line) and the single-mode prediction excluding excess noise (dotted line) well below threshold $\varepsilon_{in}=0.5\varepsilon_{th}$. For the other parameters, we have chosen $g=10^{-4}\kappa_0$, $L/f=-100$, $N=10$, giving rise to an excess-noise factor of $K\approx 1.5$.

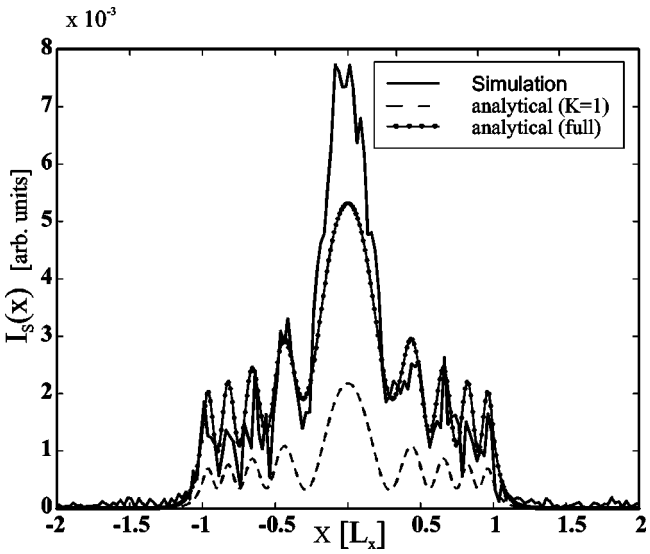

FIG. 2. Comparison of the steady-state signal intensity distribution $I(x)$ for a hard-edged unstable resonator of 100 wavelength transverse size calculated by real-space simulation (solid line) with the analytical solution Eq. (6.1) (solid line with dots) and the single-mode prediction excluding excess noise (dashed line) well below threshold $\varepsilon_{in}=0.1\varepsilon_{th}$. The parameters were chosen to give a K factor of $K\approx 2.7$ for the lowest-loss-effective eigenmode.

and $\epsilon_0=g\varepsilon_{in}/\kappa_p$. Note that the sum includes nondiagonal terms in the mode contributions, which implies interference between photon pairs generated in different mode pairs. This prevents the appearance of a simple K factor in front of the sum. Nevertheless, the intensity has a similar shape to the ground mode, but with an excess-noise enhancement. Comparing these results with our positive-P simulations, we find excellent agreement as depicted in Fig. 1.

One of the key properties of the adjoint mode matrix is that $B=A^{-1}$. However, truncating this matrix to a finite number of mode contributions strongly perturbs this property. It can be shown that using the matrix A^{-1} instead of B is numerically more accurate, although B is analytically known in principle. For this reason, we have replaced B with A^{-1} to evaluate the sums in Eq. (6.1). This numerical improvement was first found by Kostenbauder *et al.* [30] in expanding an arbitrary field distribution in nonorthogonal modes.

So far the analytical calculations, as well as the numerical results, both rely on the quasimode field expansion, the validity of which may be considered unproven. Of course, one can easily change the parameters from an unstable to a stable cavity and continuously follow the predictions. As expected, we find a perfect transition from our predictions to the well-known standard results.

As a further and more independent test of our model, we have generalized a real-space quantum simulation of the transverse dynamics in an OPO, which was developed by Gatti and coworkers [5] based on earlier work by Kolobov and Sokolov [31]. In this model a Wigner or P representation for the quantized field in real space (as opposed to mode space) is developed and stochastic field equations are derived. This model can be easily adapted to unstable cavities by simply changing the mirror curvature. Fortunately in this case we are not limited to a specific mirror or loss geometry. As a bottom line we have to simulate

$$\frac{\partial}{\partial t}A(x,t)=-\left[\Gamma(x)+i\Delta+i\frac{c^2}{2\omega}\nabla^2\right]A(x,t)+gA_pA^*(x,t)+\xi(x,t), \tag{6.3}$$

where $\Gamma(x)=\kappa(x)+i\,\delta(x)$ gives the transverse spatial dependence of the losses $\kappa(x)$ and the mirror phase shift $\delta(x)$. Here, $\xi(x,t)$ denotes a complex spatially and temporally uncorrelated white-noise source accounting for the quantum fluctuations. Its properties can be determined from the real-space Fokker-Planck equation. The details of the derivation of this equation can be found in Ref. [5].

In Fig. 2, we compare these real-space simulations with our analytical result for the case of a hard-edged resonator with negatively curved parabolic mirrors, i.e., $L/f=-1$, $L_x=L\pi$, $N=10$. The corresponding K factor for the lowest-loss quasimode for the chosen parameters is of the order of $K\approx 2.7$.

We clearly see that the results of the simulation (solid line) and Eq. (6.1) (solid line with dots) agree surprisingly well. However, the result strongly differs from a naive calculation based on effective modes but neglecting the excess-noise factor (dashed line). Note that, while the evaluation of the sum in Eq. (6.1) takes only a fraction of a second, we had to run the corresponding real-space simulation on 400-point grid for several hours to obtain only a moderate convergence of the resulting intensity distribution. The slightly higher intensity value obtained by the simulation can be attributed to the fact that no linearization assumption was used in the simulations. To check our simulation, we have also compared the case of a finite-size mirror in a stable configuration

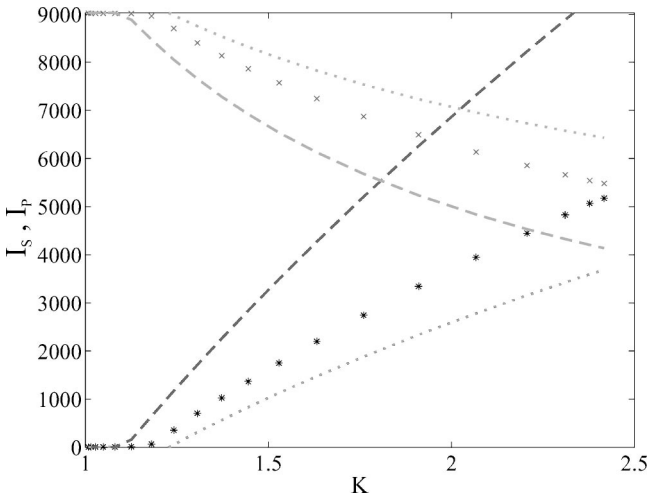

FIG. 3. Steady-state signal intensity I_S ('*') and pump intensity I_P ('x') as a function of the excess-noise-factor K for different values of the mirror curvature L/f. The pump strength is fixed at $\varepsilon_{in}=0.95\varepsilon_{th}$. We compare our results with the single-mode approximation [Eq. (5.1)] containing the full excess-noise-factor K (dashed lines) and $\sqrt{K}$ (dotted lines).

by simply reversing the mirror curvature. In this case all three curves agree almost perfectly and give the well-known results obtained by Lugiato and Marzoli [4].

VII. UNSTABLE OPO ABOVE THRESHOLD

Having demonstrated the accuracy of our method, we may now start investigating different parameter regimes. First we would like to study the influence of the excess noise on the threshold characteristics in the single-mode approximation [Eq. (5.2)]. For this purpose, we calculate the signal and pump intensities (photon numbers)

$$I_S=\sum_{nm}\langle a_n^\dagger a_m\rangle A_{nm}, \tag{7.1}$$

$$I_P=\langle A_P^\dagger A_P\rangle, \tag{7.2}$$

as a function of mirror curvature, ranging from the stable into the unstable regime ($0.2>L/f>-0.2$, $N=20$), while keeping the pump strength ε_{in} fixed at 95% of the (stable) threshold value. The horizontal axis of the plot has been rescaled to give the K factor for the chosen parameters. For the remaining parameters, we have chosen $g=0.01\kappa_0$, $\kappa_p=\kappa_0$. Figure 3 shows that one reaches the threshold where the field starts oscillating for an excess-noise factor K of approximately 1.2 that can be interpreted as an excess-noise-induced phase transition. If we compare the result with the single-mode case [Eq. (5.1)] we find that it is not the full excess noise factor but something between K and $\sqrt{K}$ that enters into the dynamics. This is indicated by the dashed and dotted lines for both pump and signal field.

Let us now explore the OPO dynamics well above threshold in more detail. If we turn on the pump at a given time $t=0$, a typical feature visible in Fig. 4 appears. The pump intensity (dashed line) grows rapidly and reaches an early

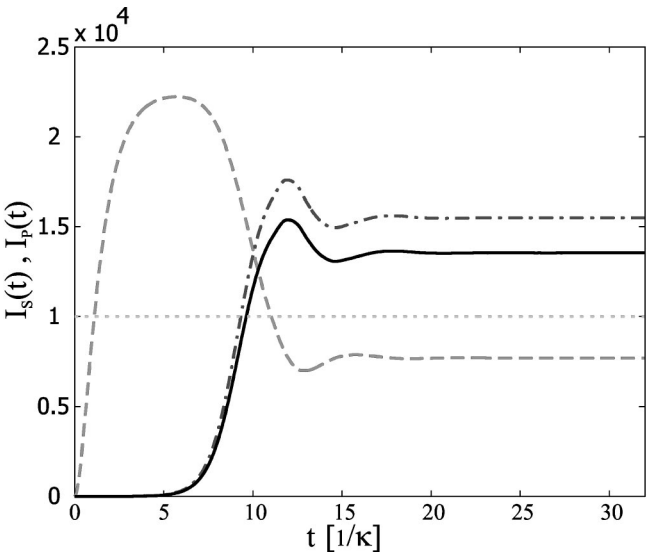

FIG. 4. The figure shows the signal intensity I_S (solid line), the pump intensity I_P (dashed line), and the contribution of the ground mode $\langle a_0^\dagger a_0\rangle$ (dash-dotted line) well above threshold $\varepsilon_{in}=1.5\varepsilon_{th}$. Compared to the stable steady-state value (dotted line) we find a clear enhancement due to excess noise ($K_0\approx 1.5$).

plateau significantly above the steady-state value. During this interval, the system exhibits a maximum of the photon pair generation via parametric amplification. Later, as the signal field builds up, pump depletion becomes important and the pump intensity decreases to its steady state in a slightly oscillatory manner. Here, we have chosen $\varepsilon_{in}=1.5\varepsilon_{th}$, $g=0.01\kappa_0$, $\kappa_P=\kappa_0$ (the rest of parameters are the same as in Fig. 2). We have considered 15 modes and summed over 10,000 stochastic trajectories. For simplicity, we have set all detunings to zero in this case. We find a clear enhancement of the signal intensity (solid line) when compared to the stable cavity result (dotted line), which can be attributed to the excess-noise factor of $K\approx 1.5$ appearing in the noise correlation term.

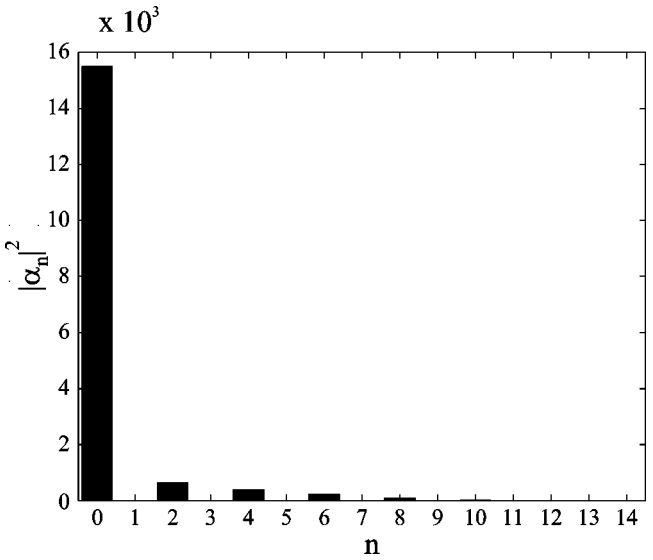

FIG. 5. The rapid decrease of higher mode coefficients, $|\alpha_n|^2=\langle a_n^\dagger a_n\rangle$, as the mode index n increases.

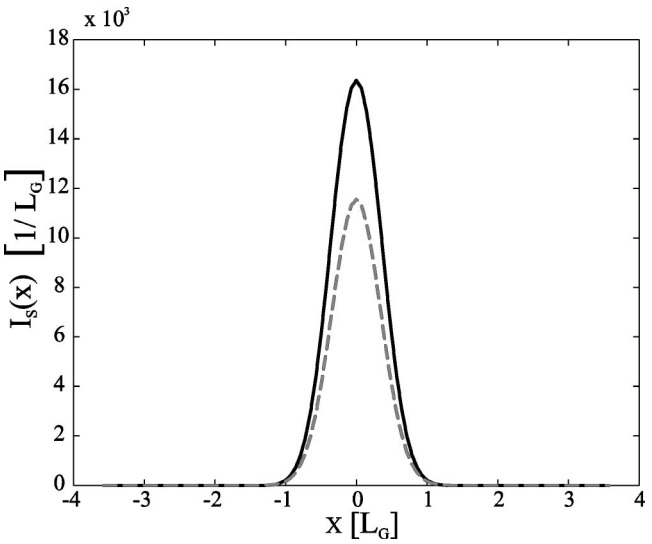

FIG. 6. The signal field $I_S(x)$ (solid line) shows an overall excess-noise enhancement and is narrowed compared to the single-mode steady-state result (dashed line) due to destructively interfering higher-mode contributions.

Interestingly, if we calculate the contribution of the lowest-order resonator mode $\langle a_0^\dagger a_0 \rangle$ (dash-dotted line in Fig. 4) to the total intensity, the result is larger than the final total sum over all modes. Although the higher-order mode contributions vanish rapidly with growing mode index (Fig. 5) they tend to interfere destructively with the ground mode. In general, this gives rise to a narrower spatial distribution of the signal intensity,

$$I_S(x) = \sum_{nm} \langle a_n^\dagger a_m \rangle u_n^* u_m . \tag{7.3}$$

This is depicted in Fig. 6 where we compare the spatial intensity distribution $I_S(x)$ (solid line) at the steady state with the stable single-mode result (dashed line).

Finally, let us now look at the photon statistics, and in particular, at the coincidence count rate,

$$g_2(0) = \frac{\langle a^\dagger a^\dagger a a \rangle}{\langle a^\dagger a \rangle^2}, \tag{7.4}$$

which is a central quantity concerning pair photon generation. This quantity is related to the probability of detecting two photons at the same time. We again find very interesting features in Fig. 7. At the moment we turn on the pump field ($t=0$), $g_2(0)$ diverges due to the well-known fact that the squeezing is growing faster than the intensity [32] ($\langle a^\dagger a \rangle \sim t^2$ and $\langle a^2 \rangle, \langle a^{\dagger 2} \rangle \sim t$). Before the signal field has significantly increased, the two-photon probability reaches a metastable state again corresponding to the regime of parametric amplification. In the regime of steady-state operation, $g_2(0)$ reduces to its coherent state value.

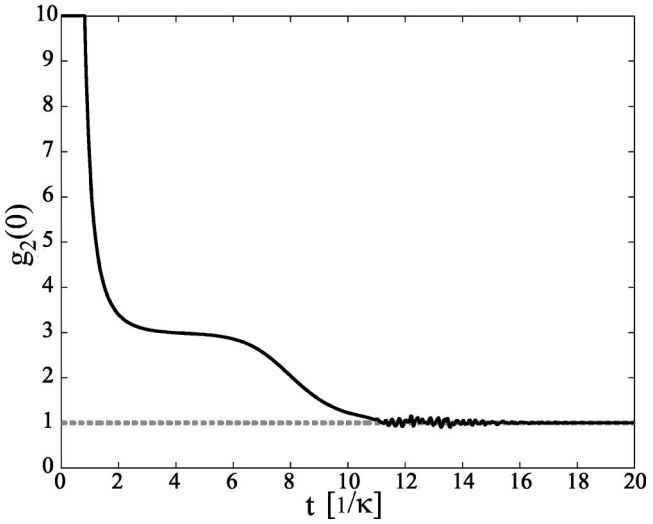

FIG. 7. The correlation function $g_2(0)$ shows a metastable state before it reaches unity at the steady state.

VIII. CONCLUSIONS

We have shown that excess noise can be expected to play an important role in parametric down conversion. Below threshold, we find a signal-intensity enhancement approximately proportional to the Petermann factor *K*. Above threshold, the enhancement factor is somewhat smaller but still important. In general, the threshold is modified and we predict a lowered oscillation threshold due to excess noise. These results are in agreement with the interpretation of parametric down conversion as a spontaneous, quantum-noise-driven process. On the other hand, the gain of intensity is accompanied by a reduction of photon pair correlation. Whereas below threshold the photons are dominantly produced in pairs, we found that the photon statistics are almost Poissonian above threshold, which of course still holds without excess noise. In the oscillation regime, higher-order mode contributions tend to interfere destructively with the lowest-order mode contribution, giving rise to a narrower effective beam width.

Although there remain some open questions in our model, there are several tests giving us strong confidence in these results. We have found excellent agreement between both of our independent numerical descriptions and the analytical treatment below threshold [18]. We have also performed the simulations in both the positive-*P* and Wigner representations, giving essentially the same predictions for low-order expectation values.

ACKNOWLEDGMENTS

We would like to thank A. S. Parkins and S. M. Tan for very helpful discussions and willing assistance. C.L. wishes to thank the Physics Department of the University of Auckland for generous hospitality. This work was supported by the University of Innsbruck, the Austrian FWF under Grant No. 13435, the University of Auckland Research Committee, and the Marsden Fund of the Royal Society of New Zealand.

[1] T. Jennewein *et al.*, Phys. Rev. Lett. **84**, 4729 (2000).
[2] M.J. Collett and C.W. Gardiner, Phys. Rev. A **30**, 1386 (1984).
[3] H. Carmichael, *An Open System Approach to Quantum Optics* (Springer-Verlag, Berlin, 1993).
[4] L.A. Lugiato and I. Marzoli, Phys. Rev. A **52**, 4886 (1995).
[5] A. Gatti *et al.*, Phys. Rev. A **56**, 877 (1997).
[6] K. Petermann, IEEE J. Quantum Electron. **15**, 566 (1979).
[7] A.E. Siegman, Phys. Rev. A **39**, 1253 (1989).
[8] W. Streifer, D.R. Scifres, and R.D. Burnham, Electron. Lett. **17**, 933 (1981).
[9] Y.J. Cheng, C.G. Fanning, and A.E. Siegman, Phys. Rev. Lett. **77**, 627 (1996).
[10] A.M. van der Lee *et al.*, Phys. Rev. A **61**, 033812 (2000).
[11] O. Emile *et al.*, Europhys. Lett. **43**, 153 (1998).
[12] P. Grangier and J.P. Poizat, Eur. Phys. J. D **7**, 99 (1999).
[13] P.J. Bardroff and S. Stenholm, Phys. Rev. A **60**, 2529 (1999).
[14] S.M. Dutra and G. Nienhuis, Phys. Rev. A **62**, 063805 (2000).
[15] C. Lamprecht and H. Ritsch, Phys. Rev. Lett. **82**, 3787 (1999).
[16] C. Lamprecht and H. Ritsch (unpublished).
[17] P.J. Bardroff and S. Stenholm, Phys. Rev. A **61**, 023806 (2000).
[18] C. Lamprecht and H. Ritsch (unpublished).
[19] Z. Ou and Y. Lu, Phys. Rev. Lett. **83**, 2556 (1999).
[20] P.D. Drummond and C.W. Gardiner, J. Phys. A **13**, 2353 (1980).
[21] M. Wolinsky and H.J. Carmichael, Phys. Rev. Lett. **60**, 1836 (1988).
[22] A. E. Siegman, *Lasers* (University Science Books, Mill Valley, CA, 1986).
[23] J.L. Doumont, P.L. Mussche, and A.E. Siegman, IEEE J. Quantum Electron. **25**, 1960 (1989).
[24] G. Barton, Ann. Phys. (Leipzig) **166**, 322 (1986).
[25] C. Cohen-Tannoudji, J. Dupont-Roc, and G. Grynberg, *Photons and Atoms* (Wiley, New York, 1996).
[26] C. W. Gardiner, *Quantum Noise* (Springer-Verlag, Berlin, 1991).
[27] P. Cohadon *et al.*, Appl. Phys. B: Lasers Opt. **66**, 685 (1998).
[28] D. F. Walls and G. J. Milburn, *Quantum Optics* (Springer-Verlag, Berlin, 1994).
[29] A.M. Van der Lee *et al.*, Phys. Rev. Lett. **81**, 5121 (1998).
[30] A. Kostenbauder, Y. Sun, and A.E. Siegman, J. Opt. Soc. Am. **14** (1997).
[31] M.I. Kolobov and I.V. Sokolov, Pis'ma Zh. Éksp. Teor. Fiz. **96**, 1945 (1989) [Sov. Phys. JETP **69**, 1097 (1989)].
[32] W. Alge, K.M. Gheri, and M.A.M. Marte, J. Mod. Opt. **44**, 841 (1997).
[33] For notational simplicity, we suppress the index of the oscillating mode in the following.